Semiconductor optical amplifiers as an optical arbitrary waveform generator for high-energy laser systems

Raphaël Humblot, Joanna De Sousa, Cyril Rapeneau, S. D. Baton, P Audebert, Frédéric Druon, Loïc Meignien

Research Article | Vol. 32, No. 22 / 21 Oct 2024 / Optics Express 37959

Optics EXPRESS

Semiconductor optical amplifiers as an optical arbitrary waveform generator for high-energy laser systems

RAPHAËL HUMBLOT,[1,2] JOANNA DE SOUSA,[1] CYRIL RAPENEAU,[1] SOPHIE BATON,[1] PATRICK AUDEBERT,[1] FRÉDÉRIC DRUON,[2] AND LOÏC MEIGNIEN[1,*]

[1]*LULI, CNRS, École Polytechnique, CEA, Sorbonne Université, Institut Polytechnique de Paris, 91128 Palaiseau CEDEX, France*
[2]*Université Paris-Saclay, Institut d'Optique Graduate School, CNRS, Laboratoire Charles Fabry, 91127 Palaiseau, France*
[*]*loic.meignien@ploytechnique.edu*

Abstract: A simple and straightforward technique is presented as a novel temporally controllable front-end for nanosecond very-high energy laser systems. It is based on an original utilization of a semiconductor optical amplifier (SOA) used as an intensity modulator. The essential characteristics of the component are analyzed in order to evaluate potential limitations. Various parameters of interest for standard operation are displayed, demonstrating its usability and its effectiveness. We demonstrate arbitrary and controllable pulse temporal profiles with duration ranging from 1 nanosecond to 100 nanoseconds and a temporal precision of 1.1 ns. A high extinction ratio is also achieved ensuring a modulation contrast up to 53 dB. The SOA is then integrated into an existing operating system in an ultra-compact, reliable all-fibered system. It is used to seed a 2*200 J laser system, exhibiting excellent performance, and validating its usability under operation conditions without any detrimental effects.

1. Introduction

The development of high-energy lasers in the nanosecond regime is a subject of significant interest for numerous scientific and industrial applications. These lasers enable precise energy deposition on targets with high temporal and spatial concentration. Lasers ranging from the 100s of mJ energy level and beyond are used for material treatment processes [1], enhancing metal resistance to deformation and corrosion. Additionally, they are also the most widely used pump source for Ti:Sa femtosecond [2,3] and OPCPA [4,5] laser amplifiers. Laser sources with energy levels ranging from the joule level up to several kilojoules find application in plasma physics and shock physics experiments, as they allow generation of extreme pressure and temperature conditions during short amount of time [6,7]. Recent advancements have shown that combining hundreds of kilojoule class lasers is one of the most promising ways for achieving controllable nuclear fusion by inertial confinement fusion [8].

Laser sources for the aforementioned applications are mainly based on a moderate-energy front end followed by increasing amplifiers (in size and in energy). The temporal properties of the entire chain are usually imposed by its front end. Two classical front-end architectures are typically used: energetic Q-switch lasers or low-energy modulated seeder. Q-switched lasers are the easiest way of achieving high energies with a simple optical configuration and good extraction efficiency. However, the properties of the output laser beam can be hard to control. In particular, the temporal profile of the laser, and with that, the energy deposition through time on target, is largely determined by the cavity geometry, the pumping power, and the gain medium. Several temporal profiles of interest are therefore inaccessible with this kind of design. On the other hand,

#530119 https://doi.org/10.1364/OE.530119
Journal © 2024 Received 14 May 2024; revised 5 Jul 2024; accepted 8 Jul 2024; published 7 Oct 2024

Optics EXPRESS

a low-energy laser impulsion (seed) with tailored properties can be subsequently amplified to reach the desired energy. Most of the properties of the output high energy pulses are then mainly dependent on the seeders and are easily controllable at low energy. In particular, it is possible to control the output pulse temporal profile using several modulation techniques while taking into account the gain saturation compensation in the amplifiers [9]. Despite a higher complexity, the controllable seeders offer more versatility than Q-switched lasers and are often required or preferred for several applications such as dynamic shock compression [10], damage threshold testing [11], laser material processing [12] or diverse parametric study of laser matter interaction and nonlinear effects in the transient regime. Several components and techniques are available in the literature to perform temporal modulation [13–21]. The main characteristics of interest sough after each of these components are the following: The modulation speed of a component defines the pulse shape accuracy and the minimal rise and fall time of the generated temporal shapes. For some applications, the requirements range from a few nanoseconds down to a hundred picosecond. The modulation contrast characterizes the difference between the minimal and maximal power achievable and should be maximized. The components spectral properties are also significant and to be considered since applications can demand either narrow spectrum properties [16], or broader bandwidth. To date, the solution used in most high energy laser facilities consists of acousto-optic modulators (AOM) and electro-optics modulators (EOM) placed in series. AOMs present high contrast (70 dB) with slow modulation time (10 ns) [17,18], while EOMs are able to modulate light in the range of 35 dB with fast modulation time (100 ps). A typical oscillator using those components consists of a CW laser gated by an AOM, generating flat-top pulses of desired duration and high contrast. The light is then further modulated by one or several EOMs to reach the desired temporal shape with high modulation speed and significant contrast. Such systems have been experimentally demonstrated and present outstanding performances in many high-energy laser facilities albeit relatively high complexity and costs [19,20].

Here, we present a novel modulation technique for high energy lasers based on a Semiconductor Optical Amplifier (SOA) [22]. This component is composed of a semiconductor gain medium with anti-reflection coating at both ends. By placing it at the output of a CW laser system, the SOA acts as an amplifier when driven with current above semiconductor threshold and as a high-extinction-ratio absorber when not alimented. Combining those two modes of operation (amplifier and absorber) allows to generate arbitrary temporal pulse shapes with high contrast and address all the described applications with a cost several times lower than state-of-the-art solutions and easy implementation.

2. SOA for gain modulation

In order to use an SOA as seeder in a high energy master oscillator power amplifier system (MOPA), its properties are checked to ensure the absence of detrimental effects during the propagation of the laser pulse in the amplifiers. In this work, the SOA and driver used are a PPL512-SOA-1064 from PicoQuant which integrates an SOA-1060-90-PM-30 DB from Innolume. A schematic of the system as well as a picture of the fiber part of the system is shown in Fig. 1.

Firstly, the spectral properties are checked. In particular, two properties are deemed of significant importance: the spectral bandwidth accessibility of the component and the conservation of spectral purity. On the one hand, a large gain spectral bandwidth is crucial for broad spectrum amplification used for plasma smoothing in fusion experiments [23] or to avoid transversal stimulated Brillouin scattering in large scale optical components [24]. Large spectral bandwidth also allows for amplification of incoherent amplified stimulated emission (ASE) without spectral narrowing or FM-AM conversion. In the case of the SOA, the amplification spectrum bandwidth is measured by direct observation of the unseeded SOA's ASE in an optical spectrum analyzer (MS9740A from Anristu with 0.03 nm resolution bandwidth).

Optics EXPRESS

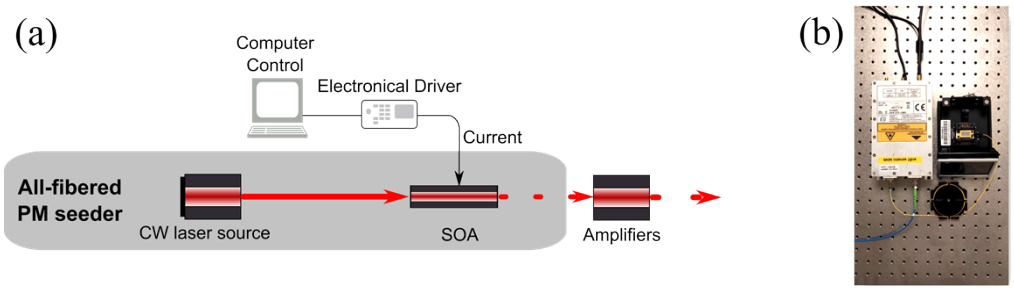

Fig. 1. (a) Schematics of an SOA used as an all-fibered temporal-shaper MOPA seeder. (b) Picture of the compact, integrated all-fibered optical arbitrary waveform generator SOA system used in this experiment. On the right, a distributed feedback narrow-linewidth (DFB) laser diode with 100 kHz linewidth and an SMSR of 45 dB, on the left, an SOA modulator. The optical signal in the seeder system is transmitted by PM980-fibers to be simply injected at the input of the chain (free space injection not shown in the picture)

The spectrum bandwidth is found to be extremely large with a FWHM of 39.2 nm as shown in Fig. 2(a). In particular, the component is compatible with the 1030 nm, 1053 nm and 1064 nm lines and is able to amplify broadband signals with an optical bandwidth well above alternative solutions. This is experimentally confirmed using a pulsed diode generating square pulses with 0.4 nm bandwidth and further modulating it using an SOA. In this case, the output spectrum shows great fidelity with the input (Fig. 2(b)). The SOA is thus able to temporally shape light with conservation of the spectrum across the pulse. While the modulation by the SOA induces dispersion, no particular artifacts in the temporal profile are measured after the shaping of this broadband pulse.

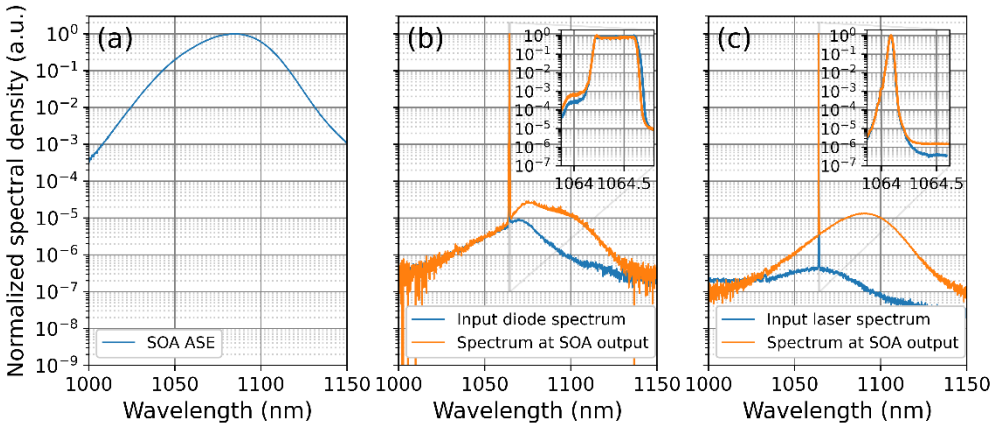

Fig. 2. Normalized spectrum measurements of (a) ASE of the SOA alimented with current of 300 mA. The shift in central wavelength versus current is negligeable (<1 nm over the full current dynamic) compared to the bandwidth of the ASE (b) Pulsed laser diode with a spectrum width of 0.42 nm FWHM at the SOA input and at the SOA output after temporal modulation (c) of the DFB laser at the SOA input and at the SOA output after temporal modulation. Both spectrum widths are below the OSA resolution of 0.03 nm

On the other hand, the conservation of the spectral purity of narrow linewidth cw injection is also important for some applications requiring interferometry. This property is measured using both a RPMC R1064SB0300 PA laser diode with side mode suppression ratio (SMSR) of 45 dB

Optics EXPRESS

and a NP Photonics fiber laser with 66 dB SMSR (shown in Fig. 2(c)). In both cases, the spectrum is measured before and after temporal modulation by the SOA. Albeit a slight degradation of the SMSR ratio of 6 dB, the spectrum remains pure, limited by the spectrometer resolution as shown in Fig. 2(c). The coherence length of the signal at system output is also tested using a custom-build Michelson interferometer and the fringes visibility stayed above 0.95 even with 1 m of optical path difference, making the SOA system compatible with most interferometric applications.

The maximum output power of the seeders is also an important consideration for high energy laser chains seeders. In particular, more input power at the seeder level allows to reduce the total gain needed in the further amplifying stages and generally improves the signal to ASE ratio of the full system. This maximum output power is determined by both the maximum input power and the maximum gain.

Firstly, the input power is limited by the saturation of the absorption of the semiconductor energy bands. While absorption-induced heating in the semiconductor medium could lead to a power acceptance of the order of few hundreds of milliwatts or more, too much input power also leads to the saturation of the absorption and a behavior close to transparency resulting in a loss of modulation contrast, as shown in Fig. 3(a). In this case, a part of the continuous wave (cw) signal starts to leak through the component and the total modulation contrast is drastically reduced. Typical input peak powers are therefore in practice limited to a few milliwatts (10 mW in our use case). Under those conditions, the absorption of the un-alimented SOA reaches 53 dB and the output power at maximum current reaches 20 mW (3 dB gain). In particular, Fig. 3(b) shows that the amplitude of the modulation capacities of the system (from maximum absorption to maximum gain) decrease with input power. The user should therefore make a compromise between the total contrast of the system and the output peak power. On the system presented in this work, an emphasis is placed on the nominal temporal profiling capacities to avoid the amplification of temporal profile artifacts.

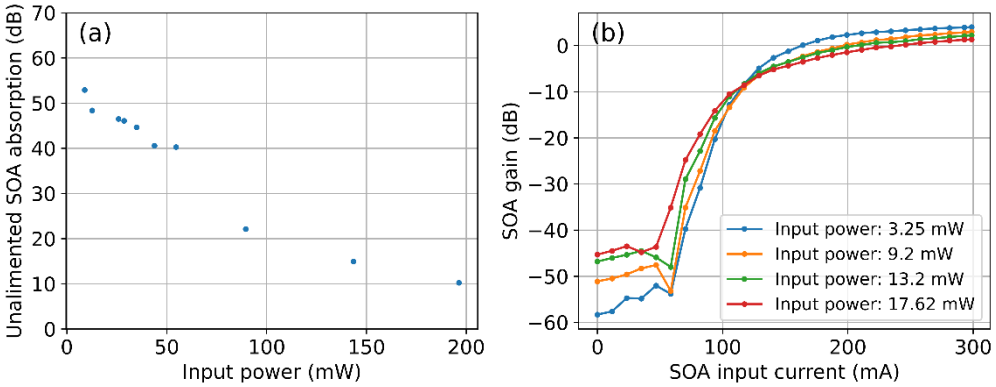

Fig. 3. (a) Maximum absorption of our SOA system. Measurements of the difference between input and output power spectra (absorption) achieved using the OSA with a span of 1 nm and a 30 pm resolution (b) Normalized output power of the SOA as a function of the driving current. The modulation capacity is above 50 dB for input powers below 10 mW and is reduced for higher input power. Input signal: CW-DFB laser diode.

The maximum available gain of the SOA also shows a trade-of. Indeed, to guaranty temporal profile purity the maximum driving current and therefore the maximum gain accessible has to be reduced. This is mainly due to the capacities of the electronic current drivers accessible that presents higher temporal accuracy for lower currents. Figure 4 shows some examples of pulse shaping in this regime with electronic driver limited to peak current of 300 mA corresponding to

Optics EXPRESS

a maximum gain of 3 dB. For alternative priority, higher output peak power using SOA (up to few hundreds of milliwatts) with good conservation of the absorption are also demonstrated by increasing the driving current as shown in Fig. 5, with another SOA and driver system. The total gain is improved to values up to 20 dB and output powers above 300 mW with peak current of 1 A, leading to 60 dB full modulation capacity (absorption + gain) corresponding to the point of the green curve Fig. 5(a). for lowest input power. This increase in gain is done at the expense of artefacts in the temporal profile (Fig. 5(b) and Fig. 5(c)). The total output power can be further improved by increasing the input power, at the cost of the total modulation capacity, both due to a gain discrepancy and absorption discrepancy.

The SOA is capable of acting either as an attenuator or an amplifier depending on the current applied. This can be useful for high-contrast pulse shaping by modulating the current. Its modulation capacities are analyzed, and several typical arbitrary temporal shapes are demonstrated. The jitter between the optical output of the component and an external asynchronous square trigger signal was limited by the electronical driver and measured to be below 66 ps RMS. The temporal resolution of the component is below 1 ns with rise and fall time as low as 1.1 ns in case of square pulses. Shapes such as square, triangle and offseted-exponential are shown in Fig. 4. The main drawback of the system is its low modulation speed compared to EOMs. This limitation is for now caused by the existing electronic drivers, which struggle to provide sharp current rise time with good temporal shape accuracy, but no measurements to find the intrinsic limitation of the SOA have been performed. However, literature from the telecommunication industry let us think going well below this limitation will prove to be difficult [25]. If needed, SOAs could be used conjointly with EOMs for easy access to high contrast and high-speed temporal shaping. The component used in this article is limited to 100 ns by the electronic driver, yet SOAs can generate modulated pulses up to tens of microsecond with nanosecond resolution. In this last case, the main limitation is the heating caused by the average current sent inside the component and the capacities of the electronic driver.

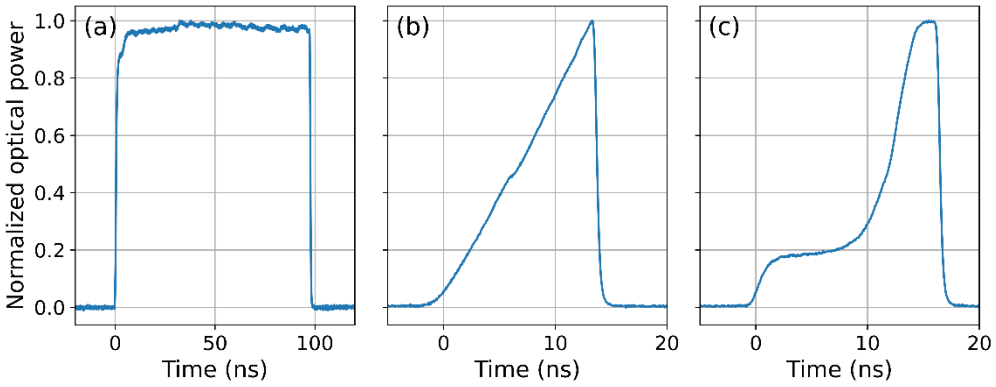

Fig. 4. Examples of temporal shapes generated with SOA modulation system with peak current limited to 100 mW. (a) 100 ns square pulse, (b) 17 ns ramp-shaped pulse and (c) 17 ns offseted-exponential pulse. Temporal shapes averaged over 4 pulses to reduce electronic noise, acquired with a 25 GHz fibered photodiode and a 20 GHz oscilloscope. Small periodic ripple oscillations are visible every 7 ns in the top of the square pulse and the ramp pulse due to residual imperfections in the driver electronical signal.

Considering the spectral properties, temporal shaping capabilities and the peak power accessible, the component is shown to be adapted to high energy laser seeding. We will then present in detail experimental outcomes of a 200 J laser chain employing an SOA as waveform-generator seeder.

Optics EXPRESS

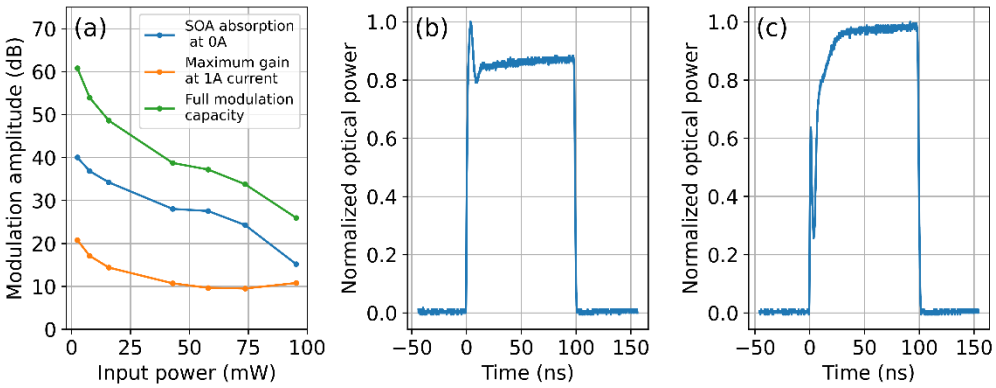

Fig. 5. Results for an SOA driven by a high current square pulse. (a) SOA isolation and gain for high current operation of 1 A. More than 300 mW of output peak power was achieved with 60 dB modulation capacity using an input power of 3 mW. The blue curve represents the same information as shown in Fig. 3(a) for a different SOA component and present the same general shape of the saturation of the absorption (b) Output temporal shape obtained at SOA output for a driving current of 500 mA of 100 ns duration. The optical pulse shape follows the current pulse shape. Command sent to the driver was square (c) Output temporal shape obtained at SOA output for a driving current of 1 A of 100 ns duration. The optical pulse shape follows the current pulse shape.

3. SOA as arbitrary waveform generator seeder in a high-energy laser system

The laser chain on which this apparatus is implemented is a 2*200 J, single-shot shot every 20 min - 1053 nm Nd:Glass laser system. This laser chain, called HERA, is currently operational at the LULI facility in Ecole Polytechnique for conducting high-energy experiments primarily for shock applications. It typically provides squared-shape laser pulses with arbitrary duration from 3 ns to 15 ns and tunable energy. Following the MOPA classical architecture, we simply modified the laser system by replacing the standard seeder by the SOA-based arbitrary waveform generator seeder. As shown in Fig. 6, it is used to inject with low energy the amplifiers of the MOPA chain. The seed pulse is then amplified to millijoule level in a Nd:YLF diode-pumped regenerative amplifier. The amplified pulse then passes through a series of additional single and double pass amplifiers of increasing size to reach the desired level of energy. The laser pulse is split at the middle of the amplification process to generate 2 separate lasers pulses that can be delayed using a delay line placed before the target chamber.

In this laser chain, the SOA is used for both temporal gating and temporal shaping. It is injected by the aforementioned laser diode providing narrow linewidth cw laser radiation. Because of the contrast properties of the SOA, the actual power of the diode is limited to 10 mW to guarantee a good optical contrast before and after the pulse. The output peak power of the fiber system after SOA amplification is therefore 20 mW. The seed pulse is then sent into a regenerative amplifier using a fiber to free space coupler. Because of the cavity length of 8 m, the maximum duration of the input pulses is limited to 17 ns (taking into account the Pockels cell rise and fall time). Since the peak power of the pulses injected in the regenerative amplifier is limited around 20 mW, the maximum seed energy is in our configuration 340 pJ. The regenerative amplifier allows to guarantee and stabilize the output energy at millijoule level without constrain on the input energy and whatever the pulse duration and shape by simply changing the number of passes in the cavity. After extraction, the contrast of the amplifier is further increased by a pulse cleaner Pockels cell removing all the ASE, pre-pulses and post-pulses leaking from the cavity with a 30 dB contrast

Optics EXPRESS

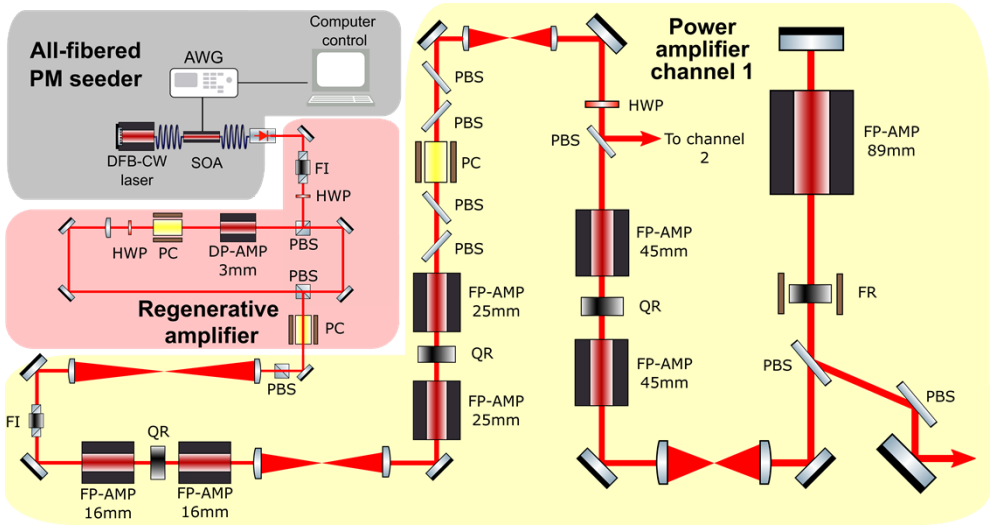

Fig. 6. Schematics of the HERA laser. AWG: Arbitrary current Waveform Generator, DFB-CW laser: DFB laser diode, SOA: Semiconductor Optical Amplifier, FI: Faraday Isolator, HWP: Half-waveplate, PBS: Polarizing Beam Splitter, DP-AMP: Diode-pumped Amplifier, PC: Pockels cell, FP-AMP: Flash-pumped Amplifier, QR: Quartz Rotator, FR: Faraday Rotator

ratio. The pulse energy after extraction and the pulse cleaner reaches 1 mJ with energy stability of 0.7% RMS before injection in the amplifying stages.

The full system reached energies above 2*200 J. The low thermal conductivity of glasses as well as the use of flash pumping reduces the repetition rate to 1 shot per 20 min at laser output. Despite the high saturation fluence of the amplifiers, the temporal saturation in the amplifier is still high. The full square pulse distortion of the system is above 70% and required pre-compensation at seeder level to reach a square pulse at output. A comparison of the input temporal profile and laser chain output is shown in Fig. 7. Output rise time is experimentally

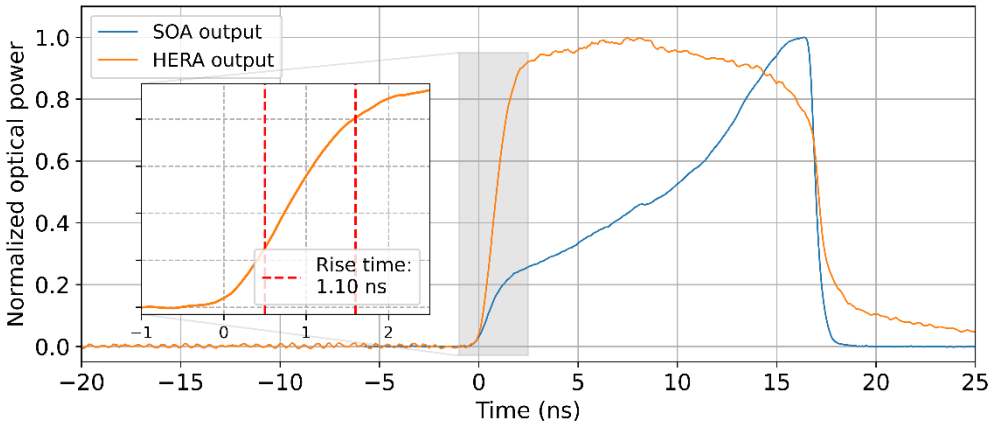

Fig. 7. Comparison of the temporal shape at the seeder level and at the laser chain output. Measures taken with an EOT-3500 photodiode and a 2 GHz bandwidth oscilloscope. Typical operation mode of the HERA laser chain producing 2*200 J square pulses.

Optics EXPRESS

measured to be 1.1 ns compatible with most shock experiments. The pulse shaping capabilities of the seeder system allow to easily tune the pulse duration from 1.5 ns (quasi-gaussian-shaped due to the limited rise and fall time) to 17 ns. Furthermore, ramp shapes and other non-standard temporal shapes are accessible with high modulation contrast. Some examples are presented Fig. 8.

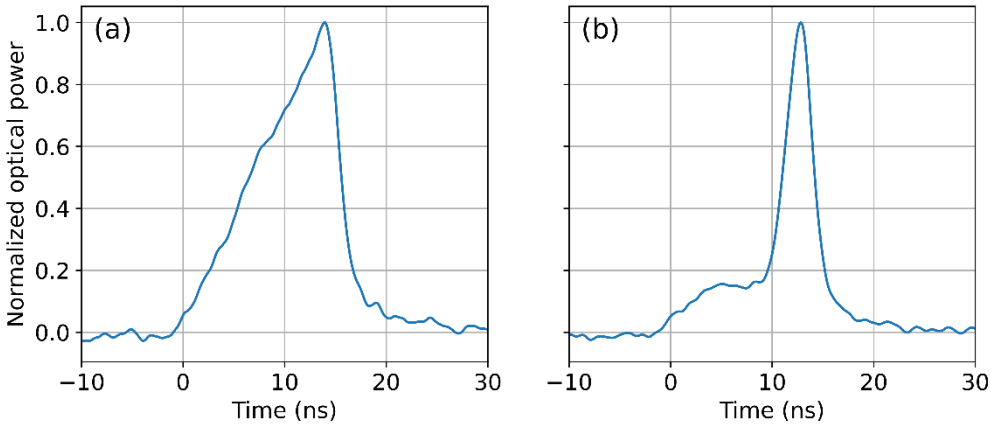

Fig. 8. Temporal shapes generated at the laser chain output using SOA temporal modulation. In those figures, 13 dB of the 53 dB of modulation dynamics have been exploited. (a) Linearly increasing ramp for shock experiments (50 J) (b) Two step temporal shape (50 J). Measures acquired using EOT-3000 photodiodes and a 2 GHz bandwidth oscilloscope.

The introduction of the beam splitting, and the 2 channels make this laser chain very flexible. The total system capabilities of 2*200 J synchronized with arbitrary temporal profiling make this laser chain compatible with a wide range of shock experiments. The SOA represents a good add-on for reaching arbitrary temporal profiles with state-of-the-art contrast as long as the rise-time requirements stays above the nanosecond time scale.

4. Conclusion and prospects

We investigated and experimentally validated the capability of the SOA component to be used as a temporal shaper seeder for high-energy laser systems employing MOPA architecture. This system is compact, user-friendly, offering over 50 dB modulation dynamic with moderate modulation speed. We demonstrate that the SOA system operates nominally with clean temporal shapes in the 10 mW peak-power range. We were able to generate arbitrary shapes from standard square to exponentially increasing peaks that presents a great interest for the plasma community. The SOA arbitrary waveform generator is ultra-compact and reliable thanks to an all-fibered architecture. Moreover, it can be easily implemented into existing laser chains as its fiber output can be injected into the laser chain without drastic modifications. We demonstrate its application on a 2×200 J system and highlight its potential. The system truly shines through its wide gain bandwidth, making it a promising choice for ICF systems requiring bandwidth in the range of several tens of nanometers. However, the main limitations of the system lie in its modulation speed and restricted peak power accessibility. Those limitations could potentially be addressed by developing new electronic drivers with higher modulation speed, higher peak current, lower jitter and cleaner temporal shapes.

Funding. Bpifrance (DOS0153842/00, DOS0153845/00); Centre National de la Recherche Scientifique.

Acknowledgments. The authors thank PicoQuant GmbH for the conjoint development of the SOAs applied to high energy laser chain seeding. The authors would like to thank all the technical teams at LULI for their valuable assistance, especially Sandra Dorard from the mechanical group.

Optics EXPRESS

Disclosures. The authors declare no conflicts of interest.

Data availability. Data underlying the results presented in this paper are not publicly available at this time but may be obtained from the authors upon reasonable request.

References

1. M. Munther, T. Martin, A. Tajyar, *et al.*, "Laser shock peening and its effects on microstructure and properties of additively manufactured metal alloys: a review," Eng. Res. Express **2**(2), 022001 (2020).
2. R. S. Nagymihály, F. Falcoz, B. Bussiere, *et al.*, "The petawatt laser of ELI ALPS: reaching the 700 TW level at 10 Hz repetition rate," Opt. Express **31**(26), 44160–44176 (2023).
3. U. Schramm, M. Bussmann, A. Irman, *et al.*, "First results with the novel petawatt laser acceleration facility in Dresden," J. Phys.: Conf. Ser. **874**, 012028 (2017).
4. N. Ekanayake, M. Spilatro, A. Bolognesi, *et al.*, "Design and optimization of a high-energy optical parametric amplifier for broadband, spectrally incoherent pulses," Opt. Express **31**(11), 17848–17860 (2023).
5. A. Wang, P. Xue, X. Liu, *et al.*, "Characteristics of broadband OPCPA based on DKDP crystals with different deuterations for the SEL-100 PW laser system," Opt. Express **32**(3), 3597–3605 (2024).
6. J. Lütgert, J. Vorberger, N. J. Hartley, *et al.*, "Measuring the structure and equation of state of polyethylene terephthalate at megabar pressures," Sci. Rep. **11**(1), 12883 (2021).
7. Y. Raffray, B. Jodar, J.-C. Sangleboeuf, *et al.*, "Zr-based metallic glasses Hugoniot under laser shock compression and spall strength evolution with the strain rate (> 107 s-1)," International Journal of Impact Engineering **181**, 104755 (2023).
8. A. B. Zylstra, O. A. Hurricane, D. A. Callahan, *et al.*, "Burning plasma achieved in inertial fusion," Nature **601**(7894), 542–548 (2022).
9. L. M. Frantz and J. S. Nodvik, "Theory of Pulse Propagation in a Laser Amplifier," J. Appl. Phys. **34**(8), 2346–2349 (1963).
10. J.-A. Hernandez, N. Sévelin-Radiguet, R. Torchio, *et al.*, "The high power laser facility at beamline ID24-ED at the ESRF," High Pressure Res. **1**, 1–28 (2024).
11. M. Veinhard, O. Bonville, S. Bouillet, *et al.*, "Parametric study of laser-induced damage growth in fused silica optics with large beams at 351 nm. Part 1: stochastic approach," Appl. Opt. **59**(31), 9643–9651 (2020).
12. A. Cournoyer, D. Gay, P. Turbis, *et al.*, "Maximizing laser ablation efficiency of silicon through optimization of the temporal pulse shape," in *Laser Applications in Microelectronic and Optoelectronic Manufacturing (LAMOM) XIX* (SPIE, 2014), Vol. 8967, pp. 125–136.
13. R. M. Malone, J. R. Bower, D. K. Bradley, *et al.*, "Imaging VISAR diagnostic for the National Ignition Facility (NIF)," in *26th International Congress on High-Speed Photography and Photonics* (SPIE, 2005), Vol. 5580, pp. 505–516.
14. K. T. Vu, A. Malinowski, D. J. Richardson, *et al.*, "Adaptive pulse shape control in a diode-seeded nanosecond fiber MOPA system," Opt. Express **14**(23), 10996–11001 (2006).
15. S. Hocquet, D. Penninckx, E. Bordenave, *et al.*, "FM-to-AM conversion in high-power lasers," Appl. Opt. **47**(18), 3338–3349 (2008).
16. R. Zhang, M. Li, J. Wang, *et al.*, "Experimental research on an arbitrary pulse generation system for imaging VISAR," Opt. Laser Technol. **43**(1), 179–182 (2011).
17. M. Beyer, J. C. Roth, E. Edwards, *et al.*, "Frequency-doubled Nd:YAG MOPA laser system with programmable rectangular pulses up to 200 microseconds," Opt. Express **29**(13), 20370–20378 (2021).
18. Q. Xiao, X. Pan, J. Guo, *et al.*, "High-stability, high-beam-quality, and pulse-width-tunable 1319 nm laser system for VISAR applications in high-power laser facilities," Appl. Opt. **59**(20), 6070–6075 (2020).
19. R. A. Meijer, A. S. Stodolna, K. S. E. Eikema, *et al.*, "High-energy Nd:YAG laser system with arbitrary sub-nanosecond pulse shaping capability," Opt. Lett. **42**(14), 2758–2761 (2017).
20. C. Dorrer, R. Roides, R. Cuffney, *et al.*, "Fiber Front End With Multiple Phase Modulations and High-Bandwidth Pulse Shaping for High-Energy Laser-Beam Smoothing," IEEE J. Sel. Top. Quantum Electron. **19**(6), 219–230 (2013).
21. A. Malinowski, K. T. Vu, K. K. Chen, *et al.*, "High power pulsed fiber MOPA system incorporating electro-optic modulator based adaptive pulse shaping," Opt. Express **17**(23), 20927–20937 (2009).
22. H. Tang, C. Yang, L. Qin, *et al.*, "A Review of High-Power Semiconductor Optical Amplifiers in the 1550 nm Band," Sensors **23**(17), 7326 (2023).
23. S. Skupsky and R. S. Craxton, "Irradiation uniformity for high-compression laser-fusion experiments," Phys. Plasmas **6**(5), 2157–2163 (1999).
24. J. R. Murray, J. R. Smith, R. B. Ehrlich, *et al.*, "Experimental observation and suppression of transverse stimulated Brillouin scattering in large optical components," J. Opt. Soc. Am. B **6**(12), 2402–2411 (1989).
25. A. Assadihaghi, H. Teimoori, and T. J. Hall, "6 - SOA-based optical switches," in *Optical Switches*, B. Li and S. J. Chua, eds., Woodhead Publishing Series in Electronic and Optical Materials (Woodhead Publishing, 2010), pp. 158–180.